Intramolecular Coulomb repulsion and anisotropies of the repulsive Coulomb barrier in multiply charged anions

Xue-Bin Wang
Department of Physics, Washington State University, 2710 University Drive, Richland, Washington 99352 and Chemical Structure and Dynamics, W. R. Wiley Environmental Molecular Sciences Laboratory, Pacific Northwest National Laboratory, MS K8-88, P.O. Box 999, Richland, Washington 99352

John B. Nicholas
Theory, Modeling, and Simulation, W. R. Wiley Environmental Molecular Sciences Laboratory, Pacific Northwest National Laboratory, MS K1-83, P.O. Box 999, Richland, Washington 99352

Lai-Sheng Wang
Department of Physics, Washington State University, 2710 University Drive, Richland, Washington 99352 and Chemical Structure and Dynamics, W. R. Wiley Environmental Molecular Sciences Laboratory, Pacific Northwest National Laboratory, MS K8-88, P.O. Box 999, Richland, Washington 99352

(Received 17 March 2000; accepted 12 April 2000)

Photoelectron spectra of the three isomers of the benzene dicarboxylate dianion (*o*-, *m*-, and *p*-BDC^{2-}) were measured in the gas phase at five photon energies. Detachment features from the carboxylate groups and the π electrons of the ring were clearly observed and distinguished. The electron binding energies were found to increase from the very small value of ~0.2 eV in *o*-BDC^{2-} to about 1.0 eV in *p*-BDC^{2-}, due to the reduced Coulomb repulsion as the two excess charges become farther apart. We found that the repulsive Coulomb barrier (RCB) for detaching electrons from the carboxylates decreases from *o*-BDC^{2-} to *p*-BDC^{2-}. However, the RCB for detaching the ring π electrons was found to be significantly higher and remain constant for the three isomers. This distinct anisotropy in the RCB involving different detachment channels is related to the different intramolecular Coulomb repulsions experienced by electrons localized on the carboxylates and the ring. Theoretical calculations were performed to obtain the equilibrium structures of both the dianions and the monoanions and to gain insight into the intramolecular electrostatic interactions. The two carboxylates in *m*- and *p*-BDC^{2-} were shown to be in-plane with the ring whereas the strong Coulomb repulsion in *o*-BDC^{2-} forces the carboxylate groups out of the plane of the ring. The theoretical results clearly show the localized nature of the excess charges on the carboxylates and help us understand the intramolecular Coulomb repulsions within the three dianions. © *2000 American Institute of Physics.* [S0021-9606(00)01426-4]

I. INTRODUCTION

Multiply charged anions (MCAs) are common in the condensed phase and play important roles in chemistry, biochemistry, and solid materials. However, MCAs have rarely been observed in the gas phase until very recently.[1–6] The strong Coulomb repulsion between the excess charges in free MCAs often make them rather fragile relative to electron autodetachment or charge-separation fragmentation in the absence of solvent or counterions. On the other hand, there exists a repulsive Coulomb barrier (RCB) against electron detachment or charge-separation fragmentation that provides dynamic stability for MCAs. In both processes the final products consist of two negatively charged particles and their long-range interaction is primarily Coulomb repulsion. Short-range binding combined with the long-range repulsion creates the RCB, which can render substantial lifetimes even for thermodynamically unstable MCAs. The RCB relative to charge-separation fragmentation has been recognized in previous theoretical studies of MCAs. Cederbaum *et al.*[2,7–16] and Simons *et al.*[4,17–21] have predicted a number of *electronically* stable free MCAs, which are in fact unstable relative to fragmentation but still possess substantial lifetimes due to the RCB. The RCB relative to electron detachment has been inferred by Compton *et al.*[1,22–24] in their investigation of doubly charged fullerene anions and others in investigation of charging effects in metal clusters.[25–29]

Recently, we developed an experimental technique to investigate gas phase MCAs using photodetachment photoelectron spectroscopy (PES) and electrospray ionization.[30–34] PES is ideal for probing the intrinsic properties of free MCAs and directly yields information about their stability,[35–43] intramolecular Coulomb repulsion,[31–43] and solvation effects.[44] We were able to directly observe the existence of the RCB against electron detachment in MCAs and estimate its magnitude.[31–43] We found profound effects of the RCB on photodetachment processes and the resulting PES spectra. In particular, we found that no photoelectrons can be observed even when a photon energy is above the binding energy of a given detachment channel, if the photon energy is below the corresponding RCB. This has now become a universal signature of PES of MCAs, rendering threshold photodetachment impossible. We were able to estimate (or bracket) the magnitude of the RCB by measuring

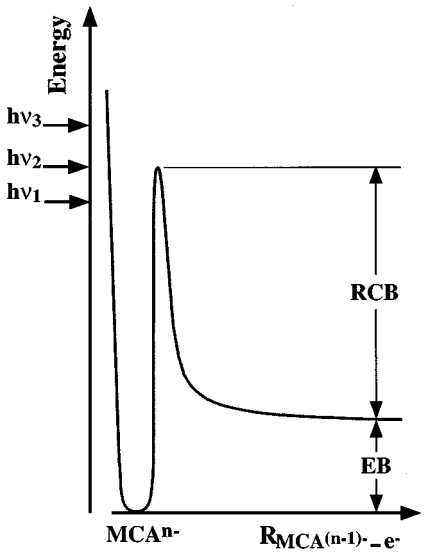

FIG. 1. Schematic potential energy curve showing the asymptotic binding energy (EB) and the repulsive Coulomb barrier (RCB) for a multiply charged anion, MCA^{n-}, and how photon-energy-dependent detachment spectra can be used to estimate the RCB (see text).

PES spectra at different photon energies. More importantly, we found that the RCB is equal in magnitude to the Coulomb repulsion between the excess charges at the equilibrium structure of an MCA. We have also observed electron tunneling effects through the RCB. Interestingly, we have been able to use the α-decay theory to semi-quantitatively interpret the electron tunneling data,[45] because the long-range repulsive Coulomb potentials are analogous between the emission of an α particle from an atomic nucleus and that of an electron from an MCA.

In our previous studies, we have used a simple, schematic one-dimensional potential curve, such as that shown in Fig. 1, to understand and represent the RCB in MCAs and its effects on the PES spectra. In reality, except for atomic species or completely spherical molecules, the RCB is expected to be complicated, multi-dimensional, and anisotropic. The RCB depicted in Fig. 1 may be considered to be along the direction of minimal Coulomb repulsion. Interestingly, Dreuw and Cederbaum have recently calculated the RCB for a linear dianion,[46] C–C–Be–C–C^{2-}, and indeed found a strong anisotropy in removing an electron from the highest occupied molecular orbital of BeC_4^{2-}.

Our estimation of the RCB from PES spectra of an MCA relies on photon-energy-dependent studies,[31–45] which are qualitatively illustrated in Fig. 1. For example, the photon energy $h\nu_1$ is below the RCB, thus there will be either no PES signals or reduced PES signals due to electron tunneling. In the tunneling regime, the normal Franck–Condon envelopes are modified by the tunneling probability for different vibrational levels, often resulting in PES bands shifted to lower binding energies.[45] This has also become a signature of PES of MCAs. At this photon energy, the RCB can be estimated to be larger than $(h\nu_1 - EB)$. On the other hand, the photon energy $h\nu_3$ is above the RCB, and in this case the RCB would be estimated to be less than $(h\nu_3 - EB)$. Hence, we can bracket the RCB: $(h\nu_1 - EB) < \mathrm{RCB} < (h\nu_3 - EB)$. If we find a photon energy $(h\nu_2)$ to be near the top of the RCB, we obtain: $\mathrm{RCB} \sim (h\nu_2 - EB)$.

Furthermore, we have found that different detachment channels, corresponding to removing electrons from different molecular orbitals (MOs) of an MCA, have their own RCBs. This should also be considered as a kind of anisotropy of the RCBs, owing to the different Coulomb repulsion experienced by individual electrons in different MOs. In principle, the individual RCBs can be estimated using tunable detachment photons. However, due to the few limited detachment laser wavelengths that we have available, we have previously assumed that the RCBs are similar for different detachment channels.[31–45] This assumption is expected to be valid for small MCAs or for removing electrons from MOs, which are mainly localized on the charge carrier groups (such as the carboxylate group, $-CO_2^-$ or sulfonate group, $-SO_3^-$).

In the current paper, we report observations of a distinct anisotropy or inequivalence of the RCBs for different detachment channels within the same MCA. We have obtained PES spectra of the three isomers of the benzene dicarboxylate dianion (*o*-, *m*-, and *p*-BDC^{2-}) and observed distinct detachment features from the carboxylates and the π electrons of the ring. Surprisingly, we found that the RCBs for detaching electrons from the carboxylate or from the ring π orbitals are quite different for each dianion. Specifically, we found that the RCBs for detachment of electrons from the carboxylate groups (the charge carriers) vary in the three isomers, corresponding to their respective intramolecular Coulomb repulsions, as expected. However, we observed that the RCBs for detachment of the ring π electrons are similar in the three isomers. Theoretical calculations were carried out to understand the structural aspect of the three dianions and help elucidate the different intramolecular Coulomb repulsions among the three isomers.

II. EXPERIMENTS

The experiments were performed with our magnetic-bottle time-of-flight PES apparatus with an electrospray source. Details have been published elsewhere[30] and only a very brief description is given here. A 10^{-4} M solution of each diacid (pH$\sim$10 by adding NaOH) in a water/methanol (2/98 volume ratio) mixed solvent was sprayed through a 0.01 mm diameter syringe needle (biased at -2.2 kV) into ambient atmosphere. The resulting charged droplets were fed into a desolvation capillary heated to $\sim$70 °C. Molecular anions formed in the desolvation capillary were guided by a radio-frequency quadrupole device into a quadrupole ion-trap. Ions were accumulated for 0.1 s in the trap before being pulsed out into the extraction zone of a time-of-flight mass spectrometer. The dominant anion signals in each case were the deprotonated species, both dianions and mono-anions. Weaker solvent complexes with one or two solvent molecules were also present. The dianion species of interest were mass-selected and decelerated before intercepted by a probe laser beam in the photodetachment zone of the magnetic-bottle photoelectron analyzer. Both a Nd:YAG laser (532, 355, and 266 nm) and an excimer laser (193 and 157 nm) were used for photodetachment in the current experiment.

Photoelectrons were collected at nearly 100% efficiency by the magnetic-bottle and analyzed in a 4 m electron flight tube. Photoelectron TOF spectra were collected and then converted to kinetic energy spectra, calibrated by the spectra of I^- and O^-. The electron binding energy spectra presented were obtained by subtracting the kinetic energy spectra from the detachment photon energies. The electron kinetic energy resolution was $\Delta E/E \sim 2\%$, i.e., 20 meV for 1 eV electrons.

III. THEORETICAL DETAILS

We used theoretical chemistry to determine the geometry and electronic structure of the three isomers of the dianion and the corresponding monoanion, and as verification of our interpretation of the PES spectra. We first optimized all the species with density functional theory (DFT). The optimizations used the hybrid B3LYP[47] exchange-correlation functional and the 6-311+G* basis set.[48] We calculated the frequencies for all species to verify that the geometries were minima on the potential energy surface. The only significant conformation flexibility involves rotation of the carboxylate groups. We explored these rotations and found only one stable conformer for each isomer of the dianion and the corresponding isomers of the monoanion.

Following the DFT optimizations, single point energies were obtained using second order Møller–Plessett perturbation theory (MP2)[49] and the 6-311+G(2*df*) basis set. The vertical detachment energy was taken as the difference in total energy between the dianion and the corresponding monoanion at the dianion geometry. The reported adiabatic detachment energy is the difference in total energy between the optimized geometries of the dianion and monoanion. All the theoretical calculations were done with GAUSSIAN98.[50]

IV. RESULTS AND DISCUSSION

A. Photoelectron spectra of *o*-BDC^{2-}, *m*-BDC^{2-}, and *p*-BDC^{2-}

The photoelectron spectra of *o*-, *m*-, and *p*-BDC^{2-} are shown in Figs. 2–4, respectively, at the five detachment photon energies. For all three dianions, we obtained rather congested spectra. Several observations can be made about the data. First, the electron binding energies increase from *o*- to *p*-BDC^{2-} as the charge separation increases (less Coulomb repulsion). The *o*-BDC^{2-} dianion is barely electronically stable with a very small electron binding energy (Fig. 2). Owing to the lack of sharp threshold features, we can only estimate the adiabatic electron detachment energies (ADEs) by comparing the spectra at different photon energies. The congested spectra also make it difficult for us to obtain the vertical detachment energies (VDEs). As we will show below, because of the RCB, higher binding energy features were cut off in the 355 nm spectra. We thus used the peak maximum in the 355 nm as the VDEs for the ground state transition and obtained estimates of the VDE as 0.47 (0.10), 1.08 (0.10), and 1.38 (0.10) eV for *o*-, *m*-, and *p*-BDC^{2-}, respectively. As we found previously and again will be discussed below, if a given photon energy is below the RCB for a given detachment transition, the PES spectrum at this photon energy cannot be used to measure the binding energy,

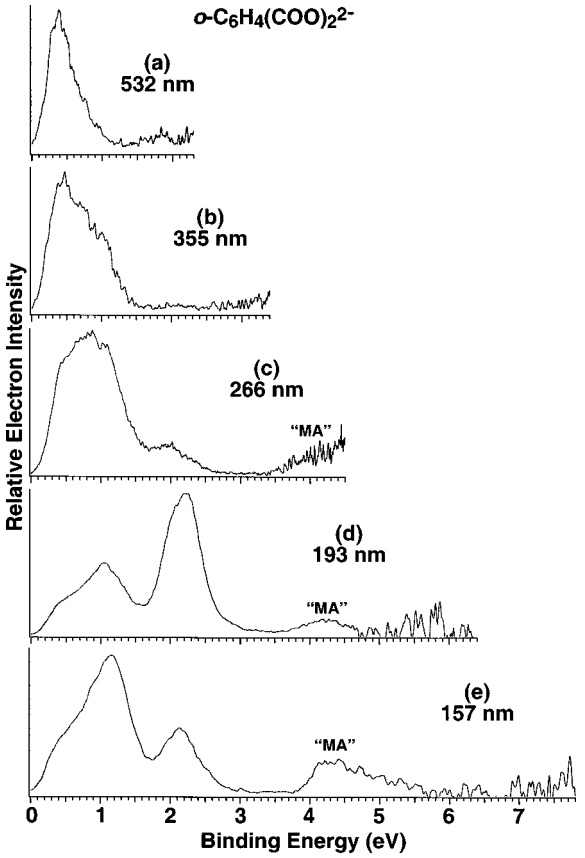

FIG. 2. Photoelectron spectra of ortho benzene dicarboxylate (*o*-BDC^{2-}) at (a) 532 nm (2.331 eV), (b) 355 nm (3.496 eV), (c) 266 nm (4.661 eV), (d) 193 nm (6.424 eV), and (e) 157 nm (7.866 eV). ''MA'' indicates features from detachment of product monoanions by a second photon.

because electron tunneling alters the normal Franck–Condon envelope for the transition. We estimated ADEs (with large uncertainties) of 0.20 (0.10), 0.85 (0.10), and 1.00 (0.10) eV for *o*-, *m*-, and *p*-BDC^{2-}, respectively, by carefully comparing the spectra at different photon energies. The estimated ADEs and VDEs are summarized in Table I. Second, all detachment features occur below 3 eV in the three dianions. The higher binding energy features (above 3.5 eV) observed in the 266, 193, and 157 nm spectra are due to detachment of singly charged anions by a second photon. These features show strong photon flux dependence. Third, the spectra for all three species show successive disappearance of higher binding energy features in the lower photon energy spectra due to the presence of the RCB, indicating the doubly charged nature of these species. These data will be used later to estimate the magnitude of the RCB.

B. Nature of the photodetachment features of the BDC^{2-} dianions

The PES spectra of *o*-BDC^{2-} show two characteristic groups of features, as seen more clearly in the 193 and 157 nm spectra (Fig. 2). The first group at lower binding energies consists of features between the threshold to about 1.6 eV. There are probably several unresolved electronic transitions in this spectral range. The second group, consisting of a broad band, is centered around 2.2 eV [Fig. 2(d)]. Interest-

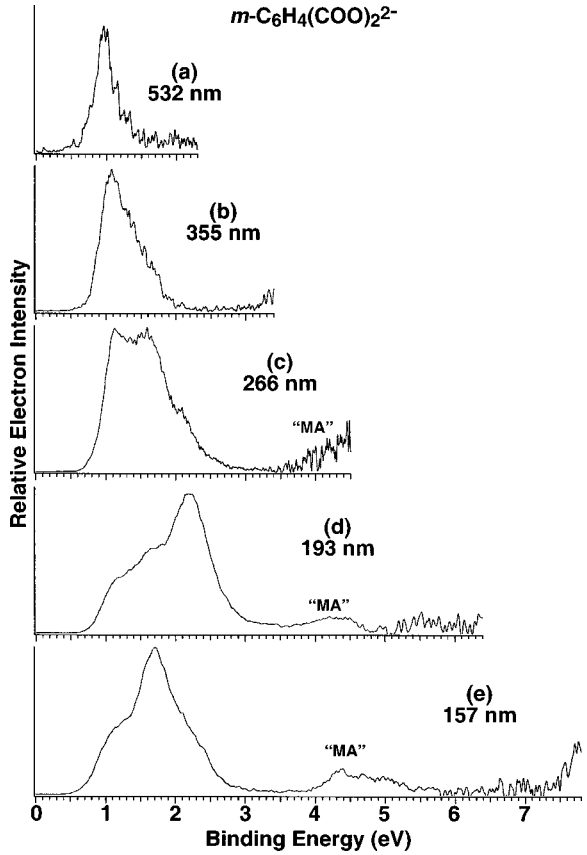

FIG. 3. Photoelectron spectra of m-BDC^{2-} at (a) 532, (b) 355, (c) 266, (d) 193, and (e) 157 nm. See Fig. 2 caption.

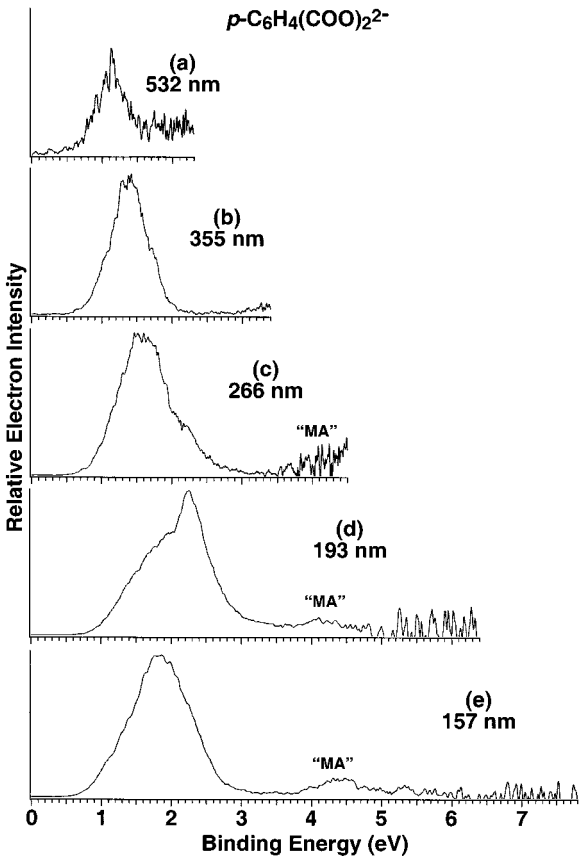

FIG. 4. Photoelectron spectra of p-BDC^{2-} at (a) 532, (b) 355, (c) 266, (d) 193, and (e) 157 nm. See Fig. 2 caption.

ingly, the same feature seems to be present in the spectra of all three dianions with nearly identical binding energies, as shown more clearly in Fig. 5(b). It appears that the first group of features is also present in the spectra of m- and p-BDC^{2-}, although they were shifted to higher binding energies, resulting in the seemingly more congested spectra in the latter cases. We attribute the first group of features to be from detachment of electrons of the carboxylate groups and the second group to be from the π system of the ring. This interpretation is reasonable, considering the fact that there is less Coulomb repulsion between the two carboxylates in m- and p-BDC^{2-} and the electron binding energies related to the carboxylates are expected to increase relative to o-BDC^{2-}. On the other hand, the Coulomb repulsion between the two negative charges (mainly localized on the carboxylates) and the π electrons of the ring is expected to be similar in the three isomers. Thus it is understandable that the binding energies of the ring π electrons would be similar in all three dianions.

To confirm our interpretation of the origin of the two groups of features in the BDC^{2-} dianions, we further performed experiments on two singly charged anions involving the carboxylate and benzene moieties. The first species is octanoate $[CH_3(CH_2)_6CO_2^-]$ with a saturated hydrocarbon chain. Its PES spectrum at 193 nm is shown in Fig. 6(a). It consists of two features, characteristic of detachment from the $-CO_2^-$ group. We have observed similar features for a series of such mono-carboxylates with different hydrocarbon chain lengths. Interestingly, we have observed similar features even for dicarboxylate dianions with saturated hydrocarbon chains [Fig. 6(b)], though at lower binding energies due to the intramolecular Coulomb repulsion. The second singly charged species that we studied is benzoate. Its spectra at 193 and 157 nm are shown in Fig. 6(c) and Fig. 6(d), respectively. The two features at the lower binding energies are similar to the features in the spectrum of octanoate and are clearly due to the $-CO_2^-$ moiety. Two additional features at higher binding energies are also observed in the spectra of benzoate and are due to detachment of the π electrons of the ring. Comparing the 193 and 157 nm spectra of benzoate, we see an obvious photon energy dependence of the different features. In particular, the intensities of the features due to the ring π systems are significantly reduced in the 157 nm

TABLE I. The experimentally estimated adiabatic [ADE (exp.)] and vertical [VDE (exp.)] electron detachment energies, RCBs, and theoretical ADE (theo.) and VDE (theo.) in eV for the three benzene dicarboxylate dianions (BDC^{2-}).

	o-BDC^{2-}	m-BDC^{2-}	p-BDC^{2-}
ADE (exp.)	0.20 (0.10)	0.85 (0.10)	1.00 (0.10)
VDE (exp.)	0.47 (0.10)	1.08 (0.10)	1.38 (0.10)
RCB(CO_2^-)	~3.0	~2.3	~1.9
RCB(π_{C6})	2.5–4.2	2.5–4.2	2.5–4.2
ADE (theo.)	−0.27	0.98	1.16
VDE (theo.)	0.47	1.14	1.30

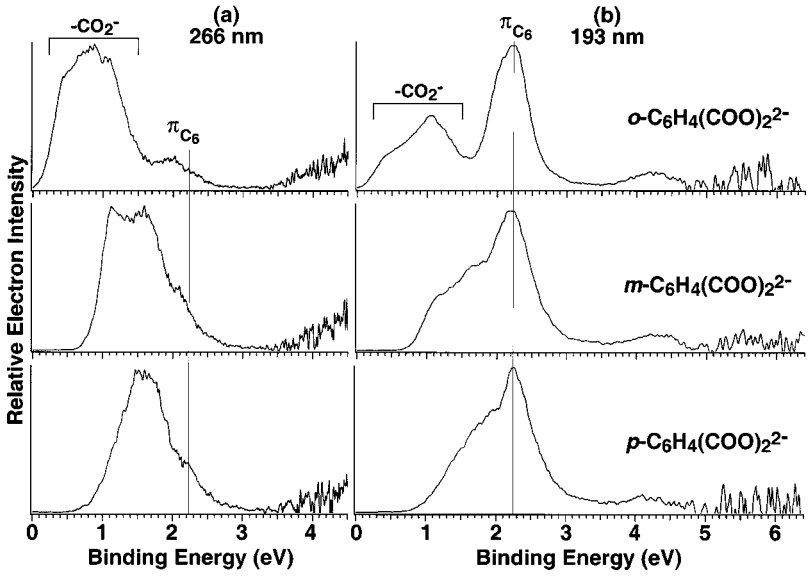

FIG. 5. Comparison of the 266 (a) and 193 nm (b) spectra of the three BDC^{2-} dianions, showing the similar binding energies of the 2.2 eV feature due to the ring π electrons (π_{C6}) in the three isomers and their change at 266 nm due to the RCB.

spectrum. We note that the 193 and 157 nm spectra of *o*-BDC^{2-} exhibit a striking similarity to the corresponding spectra of benzoate, confirming our interpretation of the origins of the PES features for the BDC^{2-} dianions.

C. Photon-energy-dependent PES and the repulsive Coulomb barriers

As shown in Fig. 1 and discussed previously, we can estimate the RCB in MCAs using PES data at different photon energies. If the detachment photon energy is near or below the RCB, the intensity of the detachment feature will be reduced due to electron tunneling. If the detachment photon energy is much below the RCB, the electron tunneling probability is very small and no photoelectron signals will be observed. However, we have to first distinguish the effects due to photon-energy-dependent detachment cross sections from those due to the RCBs. For example, the detachment feature from the ring π system in all three BDC^{2-} shows a reduced intensity in the 157 nm spectra (Figs. 2–4). This is clearly due to a reduced cross section of this detachment channel at 157 nm relative to that at 193 nm. This conclusion is confirmed by the data for benzonate at the same wavelengths (Fig. 6). In fact, the reduction of the intensity of the 2.2 eV feature significantly changed the appearance of the 157 nm spectra of *m*- and *p*-BDC^{2-} [Fig. 3(e) and Fig. 4(e)] due to overlap of the features derived from the carboxylates and the ring π system.

On the other hand, the significantly decreased intensity of the 2.2 eV feature in the 266 nm spectra [Fig. 5(a)] is due to the RCB, indicating that the 266 nm photon is lower than the RCB of this detachment channel. In general, it is easy to distinguish the RCB effects from the cross section effects. First, the RCB effects due to electron tunneling are always observed from a higher photon energy to a lower one. Second, the RCB effects always induce a shift of the PES feature to lower binding energies, as shown clearly in the 266 nm spectrum of *o*-BDC^{2-} [Fig. 5(a)]. The overlap of the 2.2 eV feature and the carboxylate-derived features makes it difficult to see the shift in the 266 nm spectra of *m*- and *p*-BDC^{2-} [Fig. 5(a)]. This spectral shift is due to the fact that in the tunneling regime the Franck–Condon profile is modified by the tunneling probability, which exponentially depends on the electron kinetic energies.[45]

Therefore, we can firmly conclude that the 266 nm photon is lower than the RCB for the detachment channel of the ring π system [designated as RCB(π_{C6})], whereas the 193 nm photon is above RCB(π_{C6}) for all three isomers. The RCB(π_{C6}) for all three isomers is then estimated to be: 2.5 eV$<$RCB(π_{C6})$<$4.2 eV. The 2.5 eV lower limit is de-

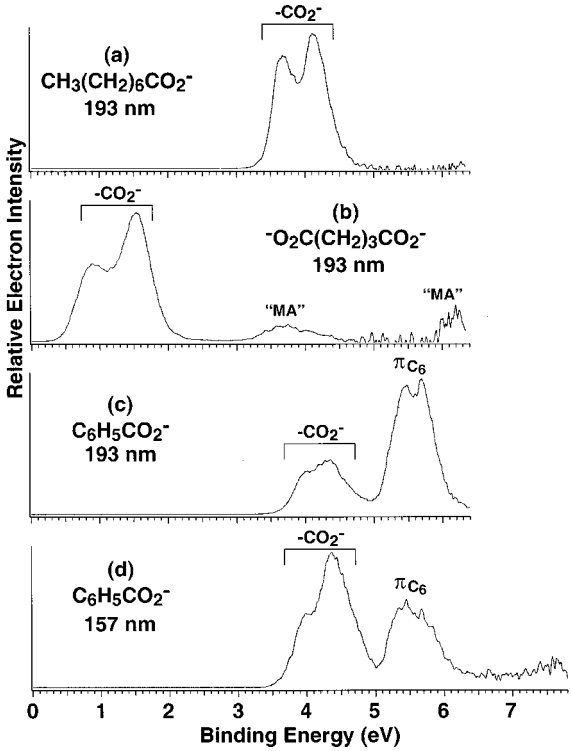

FIG. 6. Photoelectron spectra of (a) $CH_3(CH_2)_6CO_2^-$ at 193 nm, (b) $^-O_2O(CH_2)_3CO_2^-$ at 193 nm, (c) $C_6H_5CO_2^-$ at 193 nm, and (d) $C_6H_5CO_2^-$ at 157 nm.

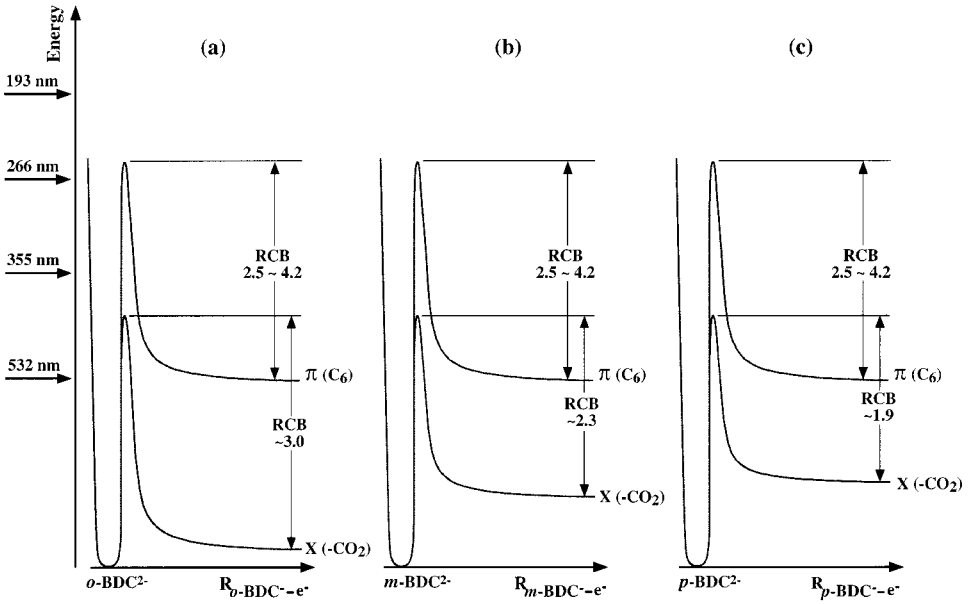

FIG. 7. Schematic potential curves showing the RCBs for detachment channels related to the carboxylates and that for the ring π electrons for (a) o-BDC^{2-}, (b) m-BDC^{2-}, and (c) p-BDC^{2-}.

rived from the 266 nm spectra (4.661 eV−2.2 eV) and the 4.2 eV upper limit is obtained from the 193 nm spectra (6.424 eV−2.2 eV). The 355 nm photon is too far below the RCB(π_{C6}), and thus the 2.2 eV feature completely disappears from the 355 nm spectra of all three BDC^{2-} dianions (Figs. 2–4). The large range of the estimate is due to the fact that the two photon energies used to derive the RCB(π_{C6}) are rather far apart. The range could be narrowed if intermediate photon energies were available. The RCB(π_{C6}) could be even more accurately determined if tunable photons were used.

The observation that RCB(π_{C6}) is similar in the three BDC^{2-} isomers is a surprise. The similarity of RCB(π_{C6}) in the three isomers suggests that the Coulomb repulsion experienced by the ring π electrons is similar in these dianions, which is evidenced in the similar binding energies of this detachment channel in all three isomers. We will show later that this can be understood based on the structures of the three dianions obtained from our theoretical calculations.

On the other hand, the Coulomb repulsion between the two excess charges in the three isomers is very different, as reflected in their different ADEs. Thus the RCBs for the detachment channels involving the carboxylate groups [designated RCB(CO_2^-)] in the three isomers are expected to vary, decreasing from o- to p-BDC^{2-}. Due to the lack of well-resolved features involving detachment of the carboxylate groups, the estimates of the RCB(CO_2^-) are more difficult. We need to make two assumptions to facilitate these estimates. First, the broad PES features from the carboxylates probably contain several detachment channels; we assume that these detachment channels all have the same RCBs. This is a reasonable assumption since the electrons removed in these cases are all from the carboxylate groups and are thus expected to experience the same Coulomb repulsion. Second, we assume that the disappearance or reduction of signal intensities from 266 to 532 nm in the spectra of all three dianions is due to the RCB, i.e., they are not due to detachment cross section effects as observed for the 2.2 eV feature between 193 and 157 nm. This assumption is also reasonable because the range of photon energy change from 266 to 355 nm and from 355 to 532 nm is not too great.

With the above two assumptions, we can estimate the RCB(CO_2^-) for each dianion on the basis of the cutoff or reduction of PES signals from the 266 to 532 nm spectra. First of all, the slight shift of the PES spectra to lower binding energies in the 532 nm spectra (more clearly seen in the m- and p-BDC^{2-} spectra) and the relatively weak PES signals suggest that the 532 nm photon is likely below the RCB(CO_2^-) for the ground state transition of all three dianions. This yields a lower limit of 2.1, 1.5, and 1.3 eV (i.e., 2.331 eV minus the threshold electron binding energy of each dianion), for the RCB(CO_2^-) of o-, m-, and p-BDC^{2-}, respectively. The 355 nm spectrum of o-BDC^{2-} [Fig. 2(b)] is cut off at about 1.2 eV, but the PES intensity begins to decrease around 0.5 eV. We thus infer that the RCB(CO_2^-)1 for o-BDC^{2-} is probably around 3.0 eV (3.496 eV−0.5 eV). The cutoff of the 355 nm spectrum of m-BDC^{2-} [Fig. 3(b)] occurs near 1.7 eV, but the spectral intensity drops precipitously starting at ~1.2 eV, resulting in an RCB(CO_2^-) of ~2.3 eV. Similarly, the spectrum of the 355 nm spectrum of p-BDC^{2-} [Fig. 4(b)] drops at ~1.6 eV, giving an RCB(CO_2^-) of ~1.9 eV for p-BDC^{2-}. All the estimated RCBs are also given in Table I and schematically shown in Fig. 7.

Therefore, we observed a systematic decrease of RCB(CO_2^-) from o- to p-BDC^{2-}. This is expected because the intramolecular Coulomb repulsion between the two excess charges, which are mainly localized on the carboxylates, decreases in this order. However, as discussed above, the RCB(π_{C6}) is quite different from these values, except for o-BDC^{2-}, for which the RCB(CO_2^-) happens to fall within the range of the RCB(π_{C6})(2.5–4.2 eV). The BDC^{2-} systems provide the first examples in which the inequivalences or anisotropies of RCBs for different detachment channels are observed. This anisotropy is due to the different intramo-

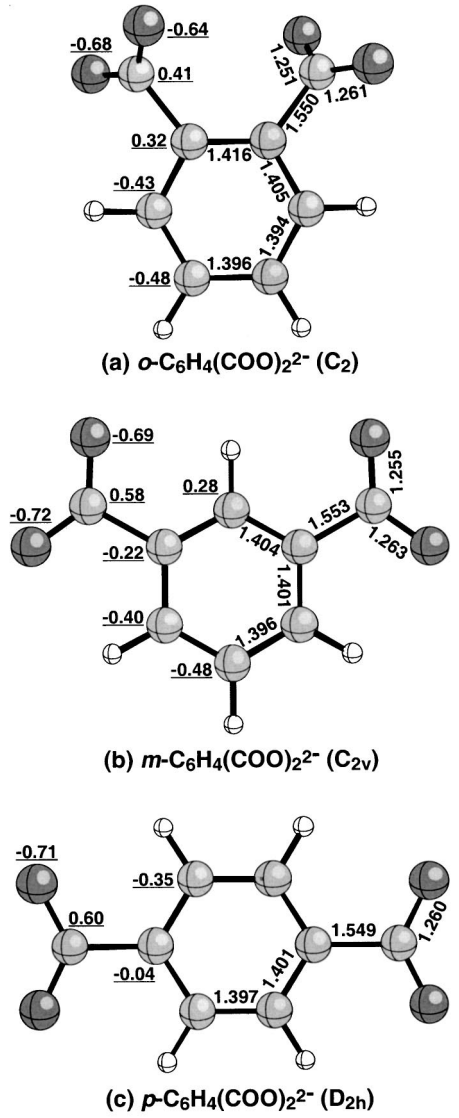

FIG. 8. Optimized (B3LYP/6-311+G*) geometries of the three isomers of BDC^{2-}. Selected bond lengths (Å) and partial charges of heavy atoms ($|e|$) (underlined) are shown.

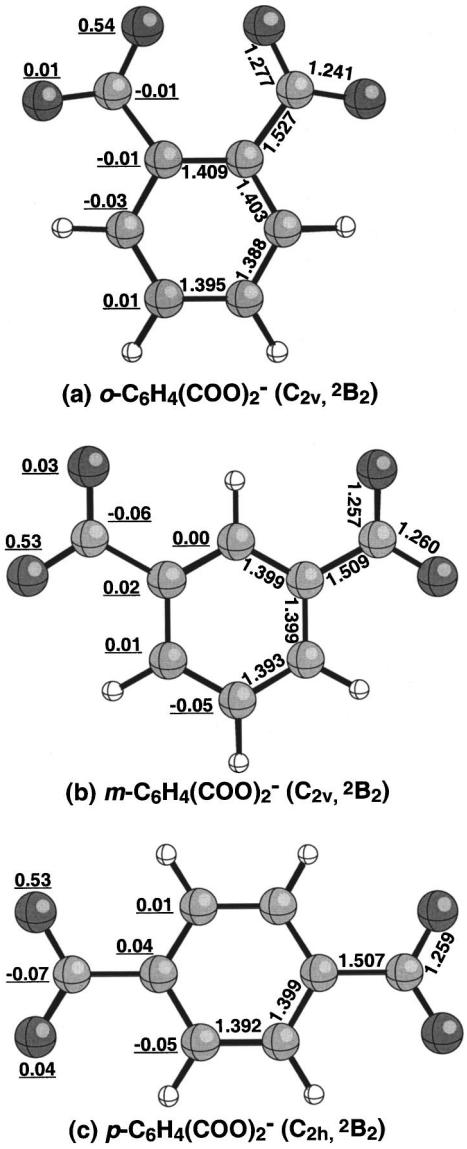

FIG. 9. Optimized (B3LYP/6-311+G*) geometries of the three isomers of the monoanion anion, BDC^{-}. Selected bond lengths (Å) and spin populations of heavy atoms (underlined) are shown.

lecular electron–electron repulsion induced by the two excess negative charges for electrons localized in different MOs. This is expected to be common for relatively large MCAs, where electrons localized in different parts of the large molecules experience different Coulomb repulsions. Thus the anisotropy of the RCB within an MCA can provide significant insight into the intramolecular electrostatic interactions. We will show next that this anisotropy in the BDC^{2-} dianions can be understood based on their structures obtained theoretically.

D. Theoretical results and structures of *o*-BDC^{2-}, *m*-BDC^{2-}, and *p*-BDC^{2-}

The optimized geometries of the dianions are shown in Fig. 8 with selected bond lengths and Mulliken Charges. We first consider *o*-BDC^{2-}. The strong electrostatic repulsion between the carboxylate groups is reflected in its geometry. For example, the optimized geometry of *o*-BDC^{2-} has C_2 symmetry [Fig. 8(a)], with the carboxylate groups rotated ~54° away from the plane of the benzene ring. In all of the other isomers, and in all the isomers of the monoanion (Fig. 9), there is less repulsion between the carboxylates, which hence maintain planarity with the ring due to conjugative interactions. The bond length between the two ring carbons to which the carboxylate groups are attached in *o*-BDC^{2-} is 1.416 Å. This is longer than any of the C–C bonds in the rings of any of the isomers. The carboxylate groups are slightly asymmetric; the two C–O bond lengths are 1.251 Å and 1.261 Å and the corresponding ∠C–C–O bond angles are 115.9° and 115.3°.

The meta isomer is planar with C_{2v} symmetry [Fig. 8(b)]. In *m*-BDC^{2-} the carboxylate groups are much farther apart than in *o*-BDC^{2-}. The C–C bond lengths within the ring are relatively uniform, ranging from 1.396 to 1.404 Å. The bond between the ring carbon to which the carboxylate is attached and the carboxylate carbon is 0.003 Å longer than

in the ortho isomer. The C–O bond lengths are also slightly longer. The ∠C–C–O bond angles are 116.7° and 115.8°. The para isomer is also planar and has D_{2h} symmetry [Fig. 8(c)]. The C–C bond lengths in the ring are even more uniform (1.397–1.401 Å), suggesting less strain on the ring with the carboxylate groups being farther apart. The carboxylate groups are now symmetric, with both C–O bond lengths being 1.260 Å and the ∠C–C–O angles being 116.2°.

The partial atomic charges from Mulliken population analyses of the MP2/6-311+G($2df$) wave functions are also given in Fig. 8. The sums of the charges on the atoms in the carboxylate groups are $-0.91|e|$ (ortho), $-0.83|e|$ (meta), and $-0.82|e|$ (para). Thus there is a slight tendency for the charge on the carboxylate group to decrease as the groups become farther apart. As expected, most of the charge of the dianions is concentrated on the oxygens.

The B3LYP/6-311+G* optimized geometries of the monoanions are shown in Fig. 9. All are planar. For the ortho isomer the C–C bond lengths in the ring are all within 0.007 Å of the corresponding bonds in the dianion. However, the C–C bond length between the ring and carboxylate carbons is much shorter (by 0.023 Å). The carboxylate groups are also more asymmetric, with C–O bond lengths of 1.241 and 1.277 Å. In the meta isomer the differences in bond distances are also small, with all bond lengths in the ring being the same as those in the dianion to within 0.005 Å. As in the ortho isomer, the bond between the ring and carboxylate carbons is much shorter (by 0.044 Å) than that in the dianion. The situation is the same for the para isomer; all bond lengths are very similar to those of the dianion except for a substantial shortening of the bond between the ring and carboxylate carbons. In this case the difference is 0.042 Å.

In Fig. 9 we also show the spin populations derived from the Mulliken analysis. The unpaired electron is shared between the carboxylate groups, but is centered on only one oxygen of each carboxylate. In the case of the ortho isomer, the spin is on the two oxygens that are closest together, while for the meta and para isomers the spin is delocalized on the two oxygens that are farthest apart. Note that the symmetry of the para isomer is C_{2h} rather than D_{2h}, which allows this spin distribution.

Finally, in Table I we also present the MP2/6-311+G($2df$)//B3LYP/6-311+G* detachment energies. The theoretical VDEs are all in excellent agreement with the experimental values. However, the theoretical results seem to underestimate the ADE of o-BDC^{2-} while overestimating the ADEs of m- and p-BDC^{2-}. For the ortho isomer, the theoretical results indicate that the monoanion is lower in energy than the dianion, resulting in a negative ADE of −0.27 eV. Nevertheless, the trend in the ADEs is consistent with the experimental values. We expect higher levels of theory [i.e., CCSD(T)] will be needed in order to duplicate better the experimental ADEs,[51] as we have shown in another recent study.[52]

E. Repulsive Coulomb barriers and the intramolecular Coulomb repulsion

As we have found before, the RCB in MCAs is equivalent to the magnitude of the intramolecular Coulomb repulsion.[31,32] As seen in Fig. 8, the excess charges in the three BDC^{2-} are localized on the carboxylates, primarily on the oxygen atoms. Thus using the optimized geometries of the dianions, we can estimate roughly the intramolecular repulsion using Coulomb's law [$e^2/4\pi\varepsilon_0 r$ or $14.4/r(\text{eV Å})$], where r can be taken as the average O–O distances on the two carboxylates. In each BDC^{2-}, there are four O–O distances which average to 4.27, 6.32, and 7.24 Å for o-, m-, and p-BDC^{2-}, respectively, giving corresponding Coulomb repulsive energies of about 3.3, 2.3, and 2.0 eV. The estimated Coulomb repulsion energies for m- and p-BDC^{2-} are in excellent agreement with the RCB(CO_2^-) values derived above from the photon-energy-dependent spectra. For o-BDC^{2-}, the simple model seems to overestimate the Coulomb repulsion. However, since the two carboxylate groups are very close in o-BDC^{2-}, small changes in the charge–charge separation result in large changes in the Coulomb energy. Furthermore, as seen in Fig. 8, the charge is not equally shared by the two oxygens in the carboxylate groups. The oxygens that are farthest apart tend to carry more charge, thus reducing the Coulomb repulsion. For example, a repulsion energy of 2.7 eV is obtained if the farthest O–O distance (5.33 Å) is used. Despite the crude, classical nature of the point-charge model, the current results are consistent with our previous observations that the RCB is equal in magnitude to the intramolecular Coulomb repulsion.

The above observations concern detachment of electrons from the charge carriers, i.e., the carboxylate groups. However, how do we understand the RCB(π_{C6}), which is related to removal of electrons other than those of the charge carriers? The similarity of the RCB(π_{C6}) among the three isomers can be understood from the optimized structures (Fig. 8), which indeed show that the carboxylates in the three isomers maintain similar distances to the ring center (~3.7 Å). The ring π electrons are then expected to experience a similar short-range repulsion [$2\times 14.4/3.7$ eV, i.e., ~7.8 eV] from the carboxylates in all the three dianions, which is the origin of the similar RCB(π_{C6}) observed.

Therefore, we have observed that, in a large MCA, different parts of the molecule will experience different Coulomb repulsions when the excess charges are localized. As we have shown before, the RCB(CO_2^-), involved in detachment of electrons from the charge carriers, is equal in magnitude to the Coulomb repulsion between the two excess charges at the equilibrium geometry. However, as we see above, the Coulomb repulsion experienced by the ring π electrons is about 7.8 eV, which is much larger than the RCB(π_{C6}) that we estimated in Sec. IV C (2.5–4.2 eV). How do we reconcile these observations? It should be pointed out that upon detachment of a ring π electron a positive hole is created. Thus the ejected electron not only will experience the Coulomb repulsion of the two negative charges, but also Coulomb attraction from the positive hole. We thus expect that the RCB will involve a combination of the repulsion and attraction at certain distance between the ejected electron and the positive hole. Therefore, the RCB in this case would be expected to be smaller than the Coulomb repulsion experienced by the ring π electrons at the equilibrium geometry.

V. CONCLUSIONS

In conclusion, we have observed that the RCB for different detachment channels of a large MCA depends on the nature or location of the electrons being detached. If the electrons are from the charge carriers, the RCB for the different channels will be similar to the intramolecular Coulomb repulsion at the equilibrium geometry of the MCA. If the electron being detached is not from the charge carrier, the RCB will be different and cannot be simply equated to the intramolecular Coulomb repulsion. We have obtained photodetachment spectra of three isomers of benzenedicarboxylate dianions. Detachment features from the carboxylates, which are the charge carriers, and the π electrons of the ring were clearly observed. We found that the RCBs for the detachment channels involving the carboxylates and the ring π electrons are different. While the RCB(CO_2^-) varies between the three isomers and is equal to the intramolecular Coulomb repulsion between the two excess charges, the RCB(π_{C6}) is relatively constant among the three isomers. The latter is understood to be due to the similar Coulomb repulsions experienced by the π electrons in the three dianions. Theoretical calculations were carried out to obtain the equilibrium structures of both the dianions and the monoanions and help understand the intramolecular electrostatic interactions.

ACKNOWLEDGMENTS

This work was supported by the National Science Foundation (CHE-9817811). Acknowledgment is also made to the Donors of the Petroleum Research Fund, administered by the American Chemical Society, for partial support of this research. Computer resources were provided by the Scientific Computing Staff, Office of Energy Research, at the National Energy Research Supercomputer Center (NERSO), Berkeley, CA. This work was performed at the W. R. Wiley Environmental Molecular Sciences Laboratory, a national scientific user facility sponsored by DOE's Office of Biological and Environmental Research and located at Pacific Northwest National Laboratory, operated for DOE by Battelle. L.S.W. is an Alfred P. Sloan Foundation Research Fellow.

[1] R. N. Compton, ''Negative ion states,'' in *Photophysics and Photochemistry in the Vacuum Ultraviolet*, edited by S. P. McGlynn *et al.* (Reidal, Netherlands, 1985).
[2] M. K. Scheller, R. N. Compton, and L. S. Cederbaum, Science **270**, 1160 (1995).
[3] J. Kalcher and A. F. Sax, Chem. Rev. **94**, 2291 (1994).
[4] A. I. Boldyrev, M. Gutowski, and J. Simons, Acc. Chem. Res. **29**, 497 (1996).
[5] G. R. Freeman and N. H. March, J. Phys. Chem. **100**, 4331 (1996).
[6] S. N. Schauer, P. Williams, and R. N. Compton, Phys. Rev. Lett. **65**, 625 (1990).
[7] H. G. Weikert, L. S. Cederbaum, F. Tarantelli, and A. I. Boldyrev, Z. Phys. D.-Atoms, Molecules, and Clusters **18**, 299 (1991).
[8] M. K. Scheller and L. S. Cederbaum, J. Chem. Phys. **99**, 441 (1993).
[9] H. G. Weikert and L. S. Cederbaum, J. Chem. Phys. **99**, 8877 (1993).
[10] M. K. Scheller and L. S. Cederbaum, J. Chem. Phys. **100**, 8934 (1994).
[11] M. K. Scheller and L. S. Cederbaum, J. Chem. Phys. **100**, 8943 (1994).
[12] M. K. Scheller and L. S. Cederbaum, J. Chem. Phys. **101**, 3962 (1994).
[13] T. Sommerfeld, M. K. Scheller, and L. S. Cederbaum, J. Chem. Phys. **103**, 1057 (1995).
[14] T. Sommerfeld, M. K. Scheller, and L. S. Cederbaum, J. Chem. Phys. **104**, 1464 (1996).
[15] V. Berghof, T. Sommerfeld, and L. S. Cederbaum, J. Phys. Chem. A **102**, 5100 (1998).
[16] A. Dreuw, T. Sommerfeld, and L. S. Cederbaum, J. Chem. Phys. **109**, 2727 (1998).
[17] A. I. Boldyrev and J. Simons, J. Chem. Phys. **97**, 2826 (1992).
[18] A. I. Boldyrev and J. Simons, J. Chem. Phys. **98**, 4745 (1993).
[19] A. I. Boldyrev and J. Simons, J. Phys. Chem. **98**, 2293 (1994).
[20] M. Gutowski, A. I. Boldyrev, J. V. Ortiz, and J. Simons, J. Am. Chem. Soc. **116**, 9262 (1994).
[21] M. Gutowski, A. I. Boldyrev, J. Simons, J. Rak, and J. Blazejowski, J. Am. Chem. Soc. **118**, 1173 (1996).
[22] R. L. Hettich, R. N. Compton, and R. H. Rotchie, Phys. Rev. Lett. **67**, 1242 (1991).
[23] C. Jin, R. L. Hettich, R. N. Compton, A. A. Tuinman, A. Derecskei-Kovacs, D. S. Marynick, and B. I. Dunlap, Phys. Rev. Lett. **73**, 2821 (1994).
[24] R. N. Compton, A. A. Tuinman, C. E. Klots, M. R. Pederson, and D. C. Patton, Phys. Rev. Lett. **78**, 4367 (1997).
[25] C. Yannouleas and U. Landman, Chem. Phys. Lett. **210**, 437 (1993).
[26] C. Yannouleas and U. Landman, Chem. Phys. Lett. **217**, 175 (1994).
[27] R. L. Martin and J. P. Ritchie, Phys. Rev. B **48**, 4845 (1993).
[28] A. Rubio, L. C. Balbas, and J. A. Alonso, Physica B **167**, 19 (1990).
[29] M. R. Peterson and A. A. Quong, Phys. Rev. B **46**, 13584 (1992).
[30] L. S. Wang, C. F. Ding, X. B. Wang, and S. E. Barlow, Rev. Sci. Instrum. **70**, 1957 (1999).
[31] L. S. Wang and X. B. Wang, J. Phys. Chem. A **104**, 1978 (2000).
[32] X. B. Wang, C. F. Ding, and L. S. Wang, Phys. Rev. Lett. **81**, 3551 (1998).
[33] L. S. Wang, C. F. Ding, X. B. Wang, and J. B. Nicholas, Phys. Rev. Lett. **81**, 2667 (1998).
[34] L. S. Wang, Comments At. Mol. Phys. (in press, 2000).
[35] C. F. Ding, X. B. Wang, and L. S. Wang, J. Chem. Phys. **110**, 3635 (1999).
[36] X. B. Wang, C. F. Ding, J. B. Nicholas, D. A. Dixon, and L. S. Wang, J. Phys. Chem. A **103**, 3423 (1999).
[37] X. B. Wang and L. S. Wang, Nature (London) **400**, 245 (1999).
[38] X. B. Wang and L. S. Wang, J. Chem. Phys. **111**, 4497 (1999).
[39] X. B. Wang and L. S. Wang, Phys. Rev. Lett. **83**, 3402 (1999).
[40] X. B. Wang, K. Ferris, and L. S. Wang, J. Phys. Chem. A **104**, 25 (2000).
[41] X. B. Wang and L. S. Wang, J. Am. Chem. Soc. **122**, 2096 (2000).
[42] X. B. Wang and L. S. Wang, J. Am. Chem. Soc. **122**, 2339 (2000).
[43] X. B. Wang and L. S. Wang, J. Phys. Chem. A **104**, 4429 (2000).
[44] C. F. Ding, X. B. Wang, and L. S. Wang, J. Phys. Chem. A **102**, 8633 (1998).
[45] X. B. Wang, C. F. Ding, and L. S. Wang, Chem. Phys. Lett. **307**, 391 (1999).
[46] A. Dreuw and L. S. Cederbaum, J. Chem. Phys. **112**, 7400 (2000).
[47] A. D. Becke, J. Chem. Phys. **98**, 5648 (1993).
[48] W. J. Hehre, L. Radom, P. v. R. Schleyer, and J. A. Pople, *Ab Initio Molecular Orbital Theory* (Wiley, New York, 1986).
[49] C. Møller and M. S. Plesset, Phys. Rev. **46**, 618 (1934).
[50] M. J. Frisch, G. W. Trucks, H. B. Schlegel, G. E. Scuseria, M. A. Robb, J. R. Cheeseman, V. G. Zakrzewski, J. A. Montgomery, Jr., R. E. Stratmann, J. C. Burant, S. Dapprich, J. M. Millam, A. D. Dániels, K. N. Kudin, M. C. Strain, O. Farkas, J. Tomasi, V. Barone, M. Cossi, R. Cammi, B. Mennucci, C. Pomelli, C. Adamo, S. Clifford, J. Ochterski, G. A. Petersson, P. Y. Ayala, Q. Cui, K. Morokuma, D. K. Malick, A. D. Rabuck, K. Raghavachari, J. B. Foresman, J. Cioslowski, J. V. Ortiz, B. B. Stefanov, G. Liu, A. Liashenko, P. Piskorz, I. Komaromi, R. Gomperts, R. L. Martin, D. J. Fox, T. Keith, M. A. Al-Laham, C. Y. Peng, A. Nanayakkara, C. Gonzalez, M. Challacombe, P. M. W. Gill, B. Johnson, W. Chen, M. W. Wong, J. L. Andres, C. Gonzalez, M. Head-Gordon, E. S. Replogle, and J. A. Pople, GAUSSIAN 98, Revision A. 4 (Gaussian, Inc., Pittsburgh, PA, 1998).
[51] We did a limited test of the effect of higher order correlation on the ADE of the ortho isomer. MP4(sdtq) single point calculations using the B3LYP/6-311+G* geometries and a modest basis set (6-31G* on H and C, 6-31+G* on O) all indicate that the monoanion is lower in energy than the dianion: MP2=−0.53 eV, MP3=−0.69 eV, MP4(d)=−0.56 eV, MP4(dq)=−0.47 eV, MP4(sdq)=−0.50 eV, and MP4($sdtq$)=−0.52 eV.
[52] P. Skurski, J. Simons, X. B. Wang, and L. S. Wang, J. Am. Chem. Soc. **122**, 4499 (2000).